Vol. 78: 187–200, 2017
https://doi.org/10.3354/ame01814

AQUATIC MICROBIAL ECOLOGY
Aquat Microb Ecol

Published online March 10

Wind drives microbial eukaryote communities in a temperate closed lagoon

Bérangère Péquin[1], Vani Mohit[1], Timothée Poisot[2], Réjean Tremblay[3], Connie Lovejoy[1,*]

[1]Département de Biologie, Québec-Océan, Institut de Biologie Intégrative et des Systèmes (IBIS), 1045 avenue de la Médecine, Université Laval, Québec G1V 0A6, Canada

[2]Québec Centre for Biodiversity Sciences and Département de Sciences Biologiques Université de Montréal, 90 Avenue Vincent d'Indy, Montréal, Québec H2V 2S9, Canada

[3]Institut des Sciences de la Mer (ISMER), Université du Québec à Rimouski, 310 Allée des Ursulines, Rimouski, Québec G5L 3A1, Canada

ABSTRACT: Phylogenetically diverse pico- (cells <2 µm diameter) and nanoplanktonic (2–20 µm) microbial eukaryotes are ubiquitous in coastal ecosystems; however, there is little understanding of the intrinsic (biological) and extrinsic (abiotic) factors that influence species composition in these communities. We investigated the microbial eukaryotes in the Havre-aux-Maisons Lagoon (Magdalen Islands, Gulf of St. Lawrence), which lacks riverine inputs and has little exchange with the surrounding gulf. We hypothesized that intrinsic successional processes and nutrient drawdown in the lagoon would lead to a decrease in average cell size over the summer. Samples for nutrients, cell concentrations from flow cytometry (FCM), and taxonomic identity using high throughput amplicon sequencing of the V4 region of the 18S rRNA gene were collected on 10 occasions between June and October 2009 and analysed in the context of physical and climatological data. Ratios of pico- to nanophytoplankton indicated no decline in average cell size over the summer, with picophytoplankton concentrations more variable. The microbial eukaryotic communities formed 3 major clusters based on phylogeny and UniFrac analysis. Taxonomically, dinoflagellates were dominant in the largest cluster, while picophytoplankton and nanoflagellates dominated the 2 other clusters. The concentrations of eukaryotic picophytoplankton increased in early summer, but decreased following periods with lower average wind speeds and increased following higher average winds. During periods with lower average wind speeds, dinoflagellates dominated. The clear impact of wind was consistent with climatological events indirectly influencing biotic interactions and picophytoplankton species composition.

KEY WORDS: Dinoflagellates · Coastal processes · Microbial community selection · 18S rRNA gene

INTRODUCTION

One of the projected effects of climate change is an increase in storm events, but predicating any relationships between storms and species or species assemblages requires basic knowledge of the taxonomic and functional makeup of marine microbial communities under a variety of conditions. Once species are known, then natural experiments can be used to test community responses to weather-related and other drivers. Normal summer production in temperate coastal regions is supported by either external nutrient inputs (Guadayol et al. 2009) or efficient nutrient recycling by microbial communities (Canton et al. 2012). The complex hydrography of most coastal regions confounds interpretation of species occurrences since communities can be rapidly replaced by advection and upwelling at a given site.

*Corresponding author: connie.lovejoy@bio.ulaval.ca

Groundwater and rivers contribute external nutrients to estuaries, while upwelling and tidal mixing are a source of nutrients to the euphotic zone in open coastal systems. These mechanisms for external nutrient input are apparently absent in the semi-closed lagoons in the Magdalen Islands, which nonetheless can support a high level of secondary production, and even aquiculture activities (Roy et al. 1991). The lagoons have limited biotic exchange with the open ocean, making them suitable for investigating the influence of weather events on successional processes, which could influence microbial eukaryotic species and potential species interactions.

The semi-closed lagoons in the Magdalen Islands Archipelago are relatively isolated, have little exchange with the adjacent Gulf of St. Lawrence, and have weak mean currents (1 to 5 cm s^{-1}) and relatively long hydraulic residence times (>20 d). Within the Havre-aux-Maisons (HAM) lagoon, water circulation is strongly influenced by the prevailing southwesterly winds that blow along the long axis from the Gulf of St. Lawrence entry point towards the outflow to the Grande-Entrée lagoon. The net result is that 2 coastal currents with a central gyre dominate the circulation in the HAM lagoon. Both the HAM and the Grande-Entrée lagoon have small, mostly sandbar catchments, with no input from rivers or streams; consequently there is little surface runoff (Koutitonsky et al. 2002, Koutitonsky 2005, Guyondet & Koutitonsky 2008). Although wind speed varies, it is nearly always present (Environment Canada; www.dfo-mpo.gc.ca), which is also evident in the windswept landscape across the Magdalen Islands. The constant wind has the effect of ensuring that the water column of the 6 m maximum depth lagoon is oxygenated to the bottom over the summer and into autumn (Mohit et al. 2014). Compared to other coastal systems, the Magdalen Islands lagoon system usually has low standing stocks of inorganic nutrients (Robert et al. 2013), and chlorophyll *a* (chl *a*) concentrations over the summer season range from 0.8 to 3 µg l^{-1} (Trottet et al. 2007). By way of contrast, chl *a* concentrations are typically >6 µg l^{-1} in other coastal systems (Gilmartin & Revelante 1978, Pennock 1985, Pérez-Ruzafa et al. 2005). In the Magdalen Islands lagoons, precipitation is the major source of external nitrate; however, most precipitation occurs in winter. Summers are relatively dry (Souchu & Mayzaud 1991, Guyondet & Koutitonsky 2008), and the influence of occasional summer rain events on phytoplankton has not been investigated.

Smaller cells, especially picophytoplankton, are favored under low nutrient conditions (Raven 1998) and it could be expected that in the absence of external nutrient inputs, the phytoplankton in the Magdalen Islands lagoons would be made up of increasingly smaller-sized cells as the summer progresses (Schapira et al. 2008, Glibert 2016). Such changes would be detected by a gradual change from a nanophytoplankton-dominated community to picophytoplankton-dominated community. Alternatively, or in addition, as the system becomes more regenerative, nanophototrophs could be replaced by heterotrophic and mixotrophic flagellate taxa (Dupuy et al. 2007). In this study, we tested the hypothesis that changes in microbial eukaryotic species composition is a result of intrinsic (biological) processes (Record et al. 2010). In this scenario, as nutrients become increasingly limiting, species that are better able to scavenge nutrients will become dominant. Specifically, we hypothesized that the community would be increasingly dominated by smaller phytoplankton. An alternative scenario would have species changes occurring as a result of external events such as storms, with no net trend towards smaller cells. Major storm events have been shown to trigger species shifts in large phytoplankton (Anglès et al. 2015) and bacterial communities (Yeo et al. 2013), but to our knowledge, the influence of local events on the whole microbial community has not been previously reported (Caron & Hutchins 2013).

In this study we first enumerated pico- and nano-sized chlorophyll-containing microbial eukaryotes and cyanobacteria using flow cytometry (FCM) to detect changes in the size structure of the photosynthetic community over time. We then investigated the microbial eukaryotic community using tagged amplicon high throughput sequencing (HTS) targeting the V4 region of the 18S rRNA gene and identified taxa to species level using a curated reference database (Lovejoy et al. 2015). Although relative frequency of HTS amplicon reads is not equivalent to cell concentrations (Blazewicz et al. 2013), comparisons of the relative number of reads of specific taxa within a community provides a window into taxonomic changes over time. We then applied multivariate statistics to test relationships between abiotic variables such as tides, salinity, temperature, wind and rain, and the dominant taxa.

MATERIALS AND METHODS

Sample collection and processing

The HAM lagoon (Magdalen Islands, Gulf of Saint Lawrence, Québec, Canada) is relatively pristine,

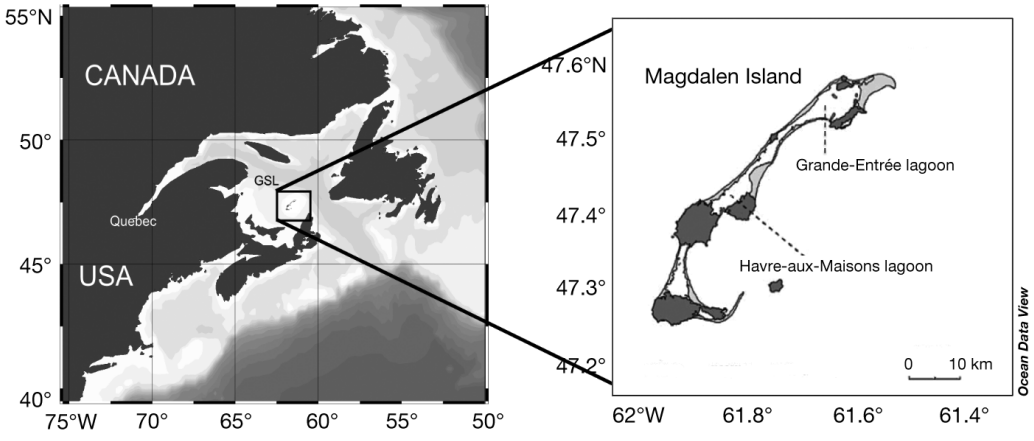

Fig. 1. Magdalen Islands, Gulf of St. Lawrence (GSL). Dark grey areas: rock; light grey regions surrounding the lagoons: sand bars

with development limited to mussel farming operations covering less than 5% of the superficial area (Myrand & Gaudreault 1995, Moisan et al. 2012). A single site (47° 25.730′ N, 61° 48.832′ W; Fig. 1) was visited approximately every 2 wk from 16 June to 8 September, and again on 6 and 20 October 2009. All sampling was done between 09:00 and 11:00 h. Temperature and salinity were recorded down the water column (5 to 6 m depth) with a Yellow Springs Instruments™ YSI 30/25 FT probe, and oxygen saturation values with a YSI 550A dissolved oxygen probe. Water samples were collected from 2.5 m below the surface using a submersible electric Rule 3700 bilge pump (Kings Pumps™) into cleaned carboys, and transported to a shore-based laboratory for filtration and processing. Duplicate water samples were taken for nutrient analysis, chl *a* and suspended particulate material (SPM). No evidence of contaminant bacteria from the sampling system was found in a companion study on attached and free-living bacteria (Mohit et al. 2014). Size fractionation is always approximate and cell breakage occurs, but since both size fractions were pooled (see below) the effects would not have had a major influence on final species detected.

Nutrient samples were pre-filtered through a 25 mm diameter 0.45 µm pore-size Millipore™ LCR membrane syringe filter into sample-rinsed 15 ml polycarbonate microtubes. Samples for chl *a* were filtered onto 25 mm diameter Whatman™ GF/F glass fiber filters. Nutrient and chl *a* samples were stored at −20°C until analysis. SPM was collected by filtering 2 l of water onto pre-combusted, pre-weighed Whatman™ GF/C filters. The filters were rinsed with a solution of ammonium formate to remove salts and then stored at −80°C until analysis. The samples for FCM were collected in 1.5 ml cryotubes following pre-filtratration through a 50 µm mesh and fixed with electron microscopy grade glutaraldehyde at a final concentration of 0.1% v/v. The cryotubes were left at room temperature in the dark for 15 min and then transferred to −80°C until processing. For DNA, 2 l of sample water was pre-filtered through a 50 µm mesh and then sequentially through a 3 µm pore size 47 mm diameter polycarbonate Millipore™ filter and a 0.2 µm pore size Sterivex™ Unit (Millipore) using a peristaltic pump system. The 3 µm filters (large fraction) were placed into cryovials with 1.8 ml of buffer (40 mM EDTA; 50 mM Tris pH = 8.3; 0.75 M sucrose). The same buffer was added to the Sterivex units (small fraction, 0.2–3.0 µm) and both fractions were immediately placed into a −80°C freezer until DNA extraction.

Laboratory procedures

Soluble reactive phosphate (SRP), soluble silicate (Si), and nitrite+nitrate were determined using standard protocols (Grasshoff et al. 2009) adapted for the AA3 Autoanalyzer (SEAL Analytical) with a detection limit of 0.01 µmol l^{-1} for each nutrient. Since nitrite concentrations are typically much less than nitrate, we use the term nitrate throughout. For chl *a*, the GF/F filters were extracted in 70°C ethanol, which allows for rapid extraction without degradation of the chl *a* (Arvola 1981, Wright et al. 2005), and concentrations were determined spectrophotometrically using a Cary 300 Bio UV-Visible spectrophotometer following an acidification step (Wright et al. 2005). The SPM filters were oven-dried at 65°C for 48 h and reweighed.

FCM concentrations of eukaryotic nanophytoplankton (nanoeuks), picophytoplankton (picoeuks), cyanobacteria, and heterotrophic bacteria were determined using a Beckmann Coulter Epics Altra™ flow cytometer equipped with a 488 nm laser beam

(of 15 mW) as described by Belzile et al. (2008). Size fraction was limited to 0.2–2.0 µm for picoeuks and 2.0–20.0 µm for nanoeuks. We distinguished cyanobacteria and eukaryotic picophytoplankton by phycoerythrin and chl *a* autofluorescence, respectively. We assumed that cyanobacteria in the pico size range were phyoerythrin-containing *Synechococcus* since a parallel study targeting 16S rRNA only detected marine *Synechococcus* in the lagoon (Mohit et al. 2014), which is consistent with the lack of freshwater phycocyanin-containing cells (confirmed by epi-fluorescence microscopy). DNA was extracted from the 3 µm PC filters and Sterivex units based on a salt extraction protocol (Aljanabi & Martinez 1997) as described by Harding et al. (2011). The extracted DNA (final DNA concentration: 35 ± 16 ng μl^{-1}) was re-suspended in TE buffer and stored at –80°C.

DNA amplification and sequencing

The extracted DNA was amplified using forward (E572F) and reverse primers (E1009R) specific to the V4 region of the 18S rRNA gene, as described in Comeau et al. (2011). The V4 region is consistently better at discriminating lower level taxa compared to other variable regions of the 18S rRNA gene in marine microbial eukaryotes (Luddington et al. 2012, Hugerth et al. 2014). To decrease potential PCR bias, for each size fraction (>3 and 0.2–3 µm) 3 separate reactions using 0.5, 1 and 2 µl of template were run and then pooled and purified using the QIAGEN QIAquick™ PCR purification kit. The concentrations of the final purified amplicons were quantified spectrophotometrically with the Nanodrop™ ND-1000. Separate multiplex identifier oligonucleotide tags (MIDs; Roche Scientific) were used for each of the 10 samples, with amplicons from large and small fractions mixed based on the proportions of picophytoplankton and nanophytoplankton estimated from flow cytometry (see Table 1). The pooled tagged amplicons were sequenced at the IBIS/Université Laval Plate-forme d'Analyses Génomiques on 1/8th plate on GS-FLX, using Titanium Chemistry (Roche Scientific). All reads from this study have been deposited in the NCBI Short Read Archive (SRA) under accession number SRP043016.

Bioinformatics analysis

Raw reads (nucleotide sequences) were processed in mothur v.1.27.0 (Schloss et al. 2009) to remove unresolved nucleotides (Ns), reads shorter than 150 nts, and sequences with one or more 7-mer or longer homopolymers. The 10 MID tags were merged and chimera checked via UCHIME (Edgar et al. 2011) in mothur. Chimeras were removed, and remaining reads were aligned against the eukaryote Silva Database (www.arb-silva.de, release 111). Following alignment, metazoan and poorly aligned reads were removed. We then used the furthest neighbor clustering option in mothur to generate operational taxonomic units (OTUs) at a similarity level of 98%. OTUs that occurred only once in the entire dataset (singletons) were removed, leaving what we termed 'high quality reads'. To facilitate comparative and statistical tests, reads from the pooled MID tags were de-multiplexed and randomly re-sampled to ensure the same number of reads from each of 10 original samples. The final number of reads (2278 per sample) used in the statistical analysis was based on the sample with the fewest 'high quality reads'. Phylogenetic similarities among eukaryotic microbial communities were assessed using weighted and normalized UniFrac distances implemented in QIIME v.1.6 (Caporaso et al. 2010). UniFrac distances were inferred from the OTU approximate maximum-likelihood phylogeny constructed in FastTree v.2.1 (Price et al. 2010). UniFrac distance clustering was computed using UPGMA, and statistical support was based on re-sampling 75% of the reads (1700) per sample and 1000 jackknife replicates.

Taxonomic identities of all reads were assigned based on a curated SS rRNA gene reference database (Lovejoy et al. 2015), which is based on the Silva taxonomy and included the Silva reference sequences. Specifically, we added representative aligned full length environmental sequences from the Scotia Shelf, North Atlantic (Dasilva et al. 2014) and the Arctic. The microbial eukaryotic reads were assigned to 196 genus-level taxa, with 121 belonging to valid taxonomic genera. These genera were binned by likely functional group based on literature reviews (Lovejoy et al. 2002, Vaulot et al. 2008). Most taxa were binned as phototrophic, mixotrophic, heterotrophic, or parasitic (Flynn et al. 2013). When making direct comparisons with the FCM data, which detects chlorophyll-containing cells, potentially mixotrophic and phototrophic taxa were combined. Dinoflagellates were binned separately since the trophic status of many dinoflagellates is not certain for many taxa (Taylor 1976, Saldarriaga et al. 2004).

Ribotypes were identified from alignments at 99% similarity excluding indels, which are the most common 454 sequencing artefact (Balzer et al. 2010, Lud-

dington et al. 2012). Abundant ribotypes defined as having >100 reads in a single sample were searched against the nr/nt database at the National Center for Biotechnology Information (NCBI) with BLAST (Altschul et al. 2009) using the NCBI parsers from BioPython (Cock et al. 2009) and an in-house python (v.2.7) script (https://gist.github.com/tpoisot/5613748). For potential harmful algal bloom (HAB) species, we constructed reference trees of the target groups to provide additional certainty in identification.

Environmental data and statistical analyses

The water level above chart datum, which is an indication of tidal level, was obtained from Fisheries and Oceans Canada (www.dfo-mpo.gc.ca). Meteorological data were collected at the HAM airport, which is 4 km from the sampling site (Environment Canada; www.climat.meteo.gc.ca). Since wind-driven currents follow a 2 to 3 d burst pattern of wind stress (Blackford 1978), we averaged wind velocities over 5 d prior to sampling to capture approximately 2 cycles prior to each sample date. The wind direction is predominantly from the southwest in summer in the Magdalen Islands (Koutitonsky 2005), and this lack of variation meant that we could not test the effect of wind direction. Total rainfall over the 5 d prior to sampling and on the day of sampling were also included as potential environmental drivers in the statistical analysis.

The community dissimilarity matrix at genus level identification was calculated using a Bray-Curtis distance matrix for principal component analysis (PCoA). We then tested the potential influence of rain, wind, salinity, temperature, oxygen, SRP, nitrate, Si, chl *a* concentration, SPM and tides on the relative abundance of ribotype reads and average phytoplankton cell size from FCM. For this, non-normal environmental data were log transformed. Ribotype reads counts with non-normal distributions were square-root transformed for the distance-based redundancy analysis (dbRDA) carried out in Canoco v.4.5 for Windows (ter Braak & Smilauer 1998). The dbRDA was realized with data from the PCoA and environmental variables. Forward selection was used to determine the most appropriate environmental variables for the dbRDA; these were temperature, Si, SPM, mean rainfall over the 5 d, mean wind speed over 5 d and tides

To determine significant associations among the functional categories, environmental variables and FCM data, we carried out Spearman's rank correlations in R v.3.1.2 (www.R-project.org). A multiple correlations correction was applied to the Type I error ($\alpha = 0.05$) with the 'p.adjust' function in R using the method of Hochberg (1988).

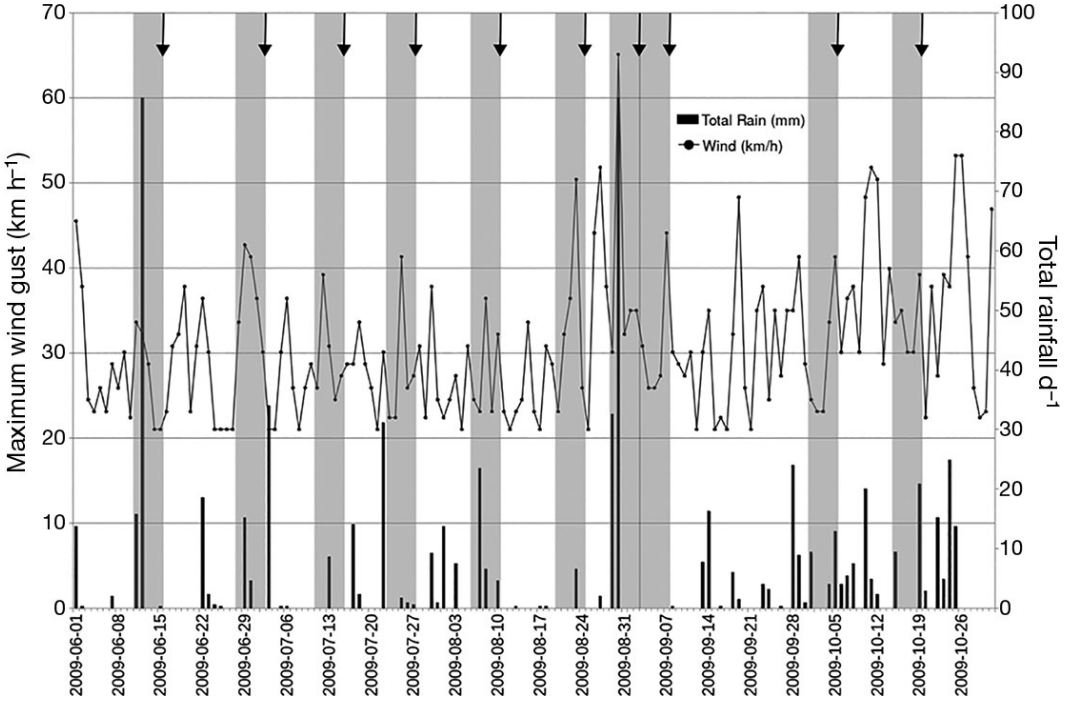

Fig. 2. Meteorological data from the airport at Havre-aux-Maisons, from 1 June to 20 October 2009. Grey bars: sampling day and the days preceding the sampling day; arrow: day of sampling; dots: daily maximum wind gusts recorded; bars: total daily rainfall. Dates given as yyyy/mm/dd

RESULTS

Environmental conditions

There were no wind-free days, with a minimum daily average wind speed of 30 km h^{-1} and a maximum of 93 km h^{-1} 4 d before the 3 September sample date (Fig. 2). At 2.5 m depth, where samples were taken, oxygen saturation ranged from 88 to 100%, with lowest values on 11 August. Temperature followed a seasonal trend, with ca. 13°C on 16 June and the highest temperature (21°C) near the end of August, then cooling to <7°C on 20 October (Table 1). Salinity varied little, with an average of 30.5 over the sampling period. The lowest salinity values were on the last date of sampling in October. Over the summer itself, rain was sporadic, with precipitation events between 0.2 and 60 mm. Minimum water level (lowest tide when we carried out sampling) was recorded on 2 July at 0.30 m above chart datum, and the highest level was 1.27 m above chart datum on 20 October (Table 1).

Nitrate concentrations in the water column varied little, with an average of 0.92 µmol l^{-1}. Silicate concentrations were more variable, with concentrations lowest in June (0.42 µmol l^{-1}) and highest on 11 and 25 August at values slightly more than 1.3 µmol l^{-1}. SRP concentrations were near the detection limit in early July and again in September, and below the detection limit on 20 October; the maximum SRP concentration was 0.45 µmol l^{-1} on 11 August. Nitrate to SRP ratios (an approximation of the Redfield ratio) varied from 2 to 95 over the summer, with no progressive seasonal trend. Chl *a* concentrations were 1.71 µg l^{-1} on 16 June, falling to a minimum of 1.1 µg l^{-1} on 16 July, then remaining nearer to 2 µg l^{-1} through late July and August. The highest value recorded was 5.69 µg l^{-1} on 6 October. SPM ranged from ca. 3.0 to 5.5 mg l^{-1}, with a minimum on 16 July (Table 1).

Community composition

Concentrations of nanoeuks were the lowest on 16 June and 20 October at around 3 × 10^3 cells ml^{-1}, with maximum concentration on 3 September, at ca. 14 × 10^3 cells ml^{-1}

Table 1. Physical and environmental variables. O_2: oxygen saturation; Temp: temperature; Rain: amount averaged over 6 d preceding the date of sampling (with maximum in parentheses); Wind: averaged over 6 d (with maximum in parentheses); Tide: height above chart datum; Nitrate: nitrate+nitrite; Si: silicate; SRP: soluble reactive phosphorus; Ratio N/P: nitrate to SRP; Chl *a*: chlorophyll *a*; SPM: total suspended particulate matter. Flow cytometry values for eukaryotic picophytoplankton (picoeuks), eukaryotic nanophytoplankton (nanoeuks), nano- and pico-sized cyanobacteria (Cyano) and bacteria are given in cells ml^{-1}. % Nanoeuks: percent of nanoeuks from the total flow cytometry (FCM) counts for all phytoplankton (eukaryotes and cyanobacteria). Standard deviation (±) is indicated for samples with replicates; –: no replicate; bd: below detection limit

	16 Jun	2 Jul	16 Jul	28 Jul	11 Aug	25 Aug	3 Sep	8 Sep	6 Oct	20 Oct
O_2 (%)	101	103.3	102.2	95	88.2	89.2	99.6	93.3	NA	101.1
Temp (°C)	13.3	15.4	18.3	19.1	19.7	21	16.2	16.6	13.1	6.7
Salinity	30.4	30.6	30.7	30.9	30.9	30.8	30.7	30.6	30.1	29.8
Rain (mm)	11.9 (60)	2.3 (10.6)	1.0 (6)	0.4 (1.2)	4.0 (16.4)	0.8 (4.6)	13.8 (60)	0.0 (0.2)	3.5 (9)	3.9 (14.6)
Wind (km h^{-1})	38 (48)	49 (61)	42 (56)	41 (59)	39 (52)	45 (72)	54 (93)	44 (63)	42 (59)	45 (56)
Tide (m)	0.69	0.30	0.76	0.75	1.13	0.88	0.96	1.17	1.26	1.27
Nitrate (µmol l^{-1})	0.98 ± 0.25	0.85	0.92 ± 0.08	0.85 ± 0.07	0.94 ± 0.05	0.93 ± 0.10	1.02 ± 0.07	0.95 ± 0.14	0.91 ± 0.00	0.86 ± 0.09
Si (µmol l^{-1})	0.42 ± 0.07	0.82	1.21 ± 0.02	0.65 ± 0.02	1.32 ± 0.11	1.34 ± 0.06	0.71 ± 0.24	1.07 ± 0.01	1.1 ± 0.22	0.55 ± 0.03
SRP (µmol l^{-1})	0.16 ± 0.04	0.03	0.20 ± 0.01	0.27 ± 0.00	0.45 ± 0.01	0.11 ± 0.04	0.03 ± 0.04	0.01 ± 0.00	0.10 ± 0.03	bd
Ratio N/P	6	28	5	3	2	8	34	95	9	–
Chl *a* (µg l^{-1})	1.71	1.24 ± 0.07	1.10 ± 0.42	1.97 ± 0.33	1.91 ± 0.45	2.02 ± 0.40	2.12 ± 0.38	1.63 ± 0.97	5.69 ± 0.30	1.65 ± 0.39
SPM (mg l^{-1})	3.10 ± 0.26	3.72 ± 0.20	3.38 ± 0.20	4.87 ± 0.29	4.47 ± 0.18	5.03 ± 0.32	5.25	5.47 ± 0.53	4.18 ± 0.08	4.14 ± 0.20
Picoeuks (×10^3)	6.60	43.4	77.8	35.2	7.29	62.7	73.1	96.4	32.8	48.9
Nanoeuks (×10^3)	3.15	8.22	7.78	9.04	8.83	6.75	14.2	7.75	9.35	3.31
Cyano (×10^3)	0.30	2.18	4.61	12.09	12.89	26.98	56.40	14.09	4.42	4.90
% Nanoeuks	31.3	15.3	8.6	16.1	30.4	7.0	9.9	6.6	20.1	5.8
Bacteria (×10^6)	1.44 ± 0.14	2.80 ± 0.44	2.30 ± 0.25	2.49 ± 0.15	3.32 ± 0.26	5.26 ± 0.40	5.18	4.42 ± 0.40	2.26 ± 0.05	2.60 ± 0.18

(Table 1). Picoeuk concentrations were $<7 \times 10^3$ cells ml^{-1} when sampling began on 16 June, and increased over 10-fold to 80×10^3 cells ml^{-1} on 16 July, back to ca. 7×10^3 cells l^{-1} on 11 August, followed by increasing concentrations between 25 August and 8 September to a maximum of 96×10^3 cells l^{-1} (Table 1). There was no consistent trend in phytoplankton cell size, estimated from the proportion of nanoeuks to total phytoplankton cell numbers (Table 1) over the sampling period. Cyanobacteria from the FCM data varied less than for picoeuks, with a more gradual increase in concentrations over summer and maximum values on 3 September. Bacteria concentrations changed little, but were slightly higher in late August and early September (Table 1).

Reads were initially classified into the major microbial eukaryote groups following Adl et al. (2012) and NCBI taxonomy. For the individual samples, alveolates accounted for 20 to 70% of the reads, Chlorophyta accounted for 5 to 40% and stramenopiles 5 to 25%. Cryptophyta and Haptophyta represented <20% of reads in any one sample. Other groups such as Centroheliozoa and Amoebozoa were rare (see Fig. S1 in the Supplement at www.int-res.com/articles/suppl/a078p187_supp.pdf). For the functional binning, Chlorophyta including the Mamiellales (*Micromonas*, *Bathycoccus* and *Ostreococcus*) accounted for the highest proportion of phototrophic and mixotrophic taxa, followed by Cryptophyceae and Prymnesiales. Other phototrophs included Zygodiscales on 16 July and Pelagophyceae in September (Fig. 3A). Ciliates and Cercozoa together accounted for 80% of the reads matching heterotrophs, uncultivated phylogenetically diverse marine stramenopiles (MASTs), katablepharids (*Katablepharis* and *Leucocryptos*) and Picozoa. Apicomplexa, Polycystinea, Labyrinthulida and Acantharia were also detected and were placed in as the 'Others' heterotrophic category (Fig. 3B).

For the dinoflagellates, 30% of the total reads were assigned the *Gymnodinium*, *Prorocentrum*, *Protoperidinium* (GPP) group (Taylor 1976, Saldarriaga et al. 2004). Among these, best BLASTn matches were primarily to *Gyrodinium helveticum*, *Karenia mikimotoi*, *Scrippsiella hangoei*, *Karlodinium* sp. and *Gyrodinium fusiforme* (Fig. 3C). *Pelagodinium béii* (Siano et al. 2010), *Gymnodinium aureolum* strain SWA (AY999082), *Nematondinium* sp. BSL_2009a (FJ947039) and *Gymnodinium catenatum* were also found. In total, 40% of the dinoflagellate reads could not be classified below the level of phyla and were grouped as unclassified dinoflagellates. These represented multiple genera and species-level OTUs (Fig. 3).

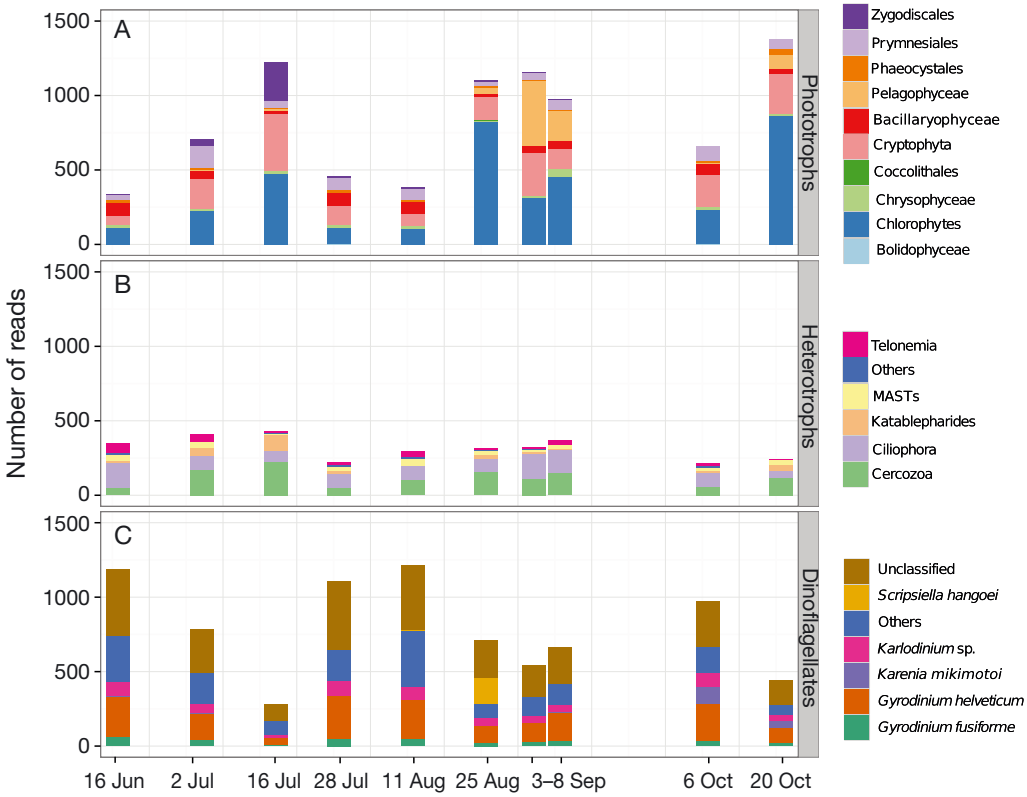

Fig. 3. Finer-level taxonomic assignation normalized reads classified as (A) phototrophs, (B) heterotrophs and (C) dinoflagellates

Abundant ribotypes, defined as those with ≥100 reads, accounted for >4.3% of reads from at least 1 sample out of the 2278 reads per sample (Table 2). All but one of these ribotypes were >98% similar to species-level taxa from culture collections or verified environmental sequences (see Table S1 in the Supplement). The single abundant ribotype that was not resolved to species level clustered within the Zygodiscales and was 96.5% similar to the genus *Braarudosphaera*; we refer to this ribotype as *Braarudosphaera*-like.

The most common ribotype in the entire normalized dataset (22780 reads) matched *G. helveticum*, accounting for 1414 reads. Eight ribotypes with single incidences of ≥4.3% of the community included *K. mikimotoi*, *S. hangoei*, *Chrysochromulina simplex*, the *Braarudosphaera*-like ribotype, *Ostreococcus lucimarinus*, *Nannochloris* sp., *Katablepharis* sp., and the picozoan (Table 2). Six of the abundant ribotypes were recovered from all samples: *G. helveticum*, *Falcomonas daucoides*, *C. simplex*, *Pyramimonas* sp., the picozoan, *Micromonas pusilla* and *Bathycoccus prasinos* (Table 2).

Initially, picoeuks were mostly in the Mamiellophyceae, but by September the pelagophyte *Aureococcus anophagefferens* dominated reads, with Mamiellophyceae once more predominant at the end of October. Although the first 3 sampling dates indicated a temporal increase in the concentration of picoeuks, this trend did not persist. In addition, no seasonal trends were detected at the whole community level using a weighted UniFrac, which takes into account phylogenetic distance within the community. The samples that had a higher proportion of picophytoplankton detected using FCM (picoeuks) on 16 July, 25 August and 20 October formed one cluster while the 3 and 8 September samples formed a second. The 5 other dates grouped into a single larger cluster dominated by dinoflagellate reads (Fig. 4). The unweighted UniFrac showed the same grouping (data not shown).

Drivers of the community changes over time

Associations among the communities clustered by abundant ribotype and environmental variables were examined using distance-based redundancy analysis (dbRDA). The first axis explained 55% of total variance and separated sampling dates that were dominated by picoplankton taxa from the rest, with wind and Si concentrations having the greatest influence. The second axis explained 18.5% of total variance and separated communities mostly associated with temperature (Fig. 5). In total, 94% of the variance could be explained using 6 significant factors on 4 axes. A dbRDA, run using whole communities where the matrix included all OTUs as input, followed the same clustering (data not shown).

Table 2: Abundant ribotypes on each sampling date number of reads out of a total number of reads out of 2278 per date. Full taxonomic names and accession numbers for the best matches are given in Table S1 in the Supplement at www.int-res.com/articles/suppl/a078p187_supp.pdf. Category (CAT) of row refers to Fig. 4, Category taxa is by functional group: Dino: dinoflagellate; MNF: mixotrophic nanoflagellate; PPP: picophytoplankton; PPP-?: uncertainty of size; HNF: heterotrophic nanoflagellate; HPF: heterotrophic picoflagellate; Para: putative parasite; Pico 1: dominated by chlorophyte species; Pico 2: dominated by *Aureococcus anophagefferens*

Species	CAT	16 Jun Dino	2 Jul Dino	16 Jul Pico1	28 Jul Dino	11 Aug Dino	25 Aug Pico1	3 Sep Pico2	8 Sep Pico2	6 Oct Dino	20 Oct Pico1
Gyrodinium helveticum	Dino	191	140	33	237	211	89	94	147	190	82
Karenia mikimotoi	Dino	0	0	1	0	0	5	0	1	116	46
Scrippsiella hangoei	Dino	0	1	0	0	7	172	1	0	0	0
Falcomonas daucoides	MNF	32	104	142	23	19	103	161	62	165	47
Chrysochromulina simplex	MNF	37	144	45	69	61	29	37	67	71	59
Pyramimonas sp.	MNF	22	64	176	39	57	70	62	100	44	55
Braarudosphaera	PPP-?	0	41	257	7	4	7	0	0	0	0
Micromonas pusilla	PPP	38	59	93	36	24	183	101	151	85	93
Bathycoccus prasinos	PPP	27	20	95	21	1	80	23	41	28	145
Ostreococcus lucimarinus	PPP	5	25	3	0	0	2	0	2	32	306
Nannochloris sp.	PPP	0	0	7	1	0	143	10	6	1	2
Picochlorum sp.	PPP	2	16	46	2	0	127	70	90	10	135
Aureococcus anophagefferens	PPP	0	2	8	5	3	41	437	202	5	96
Picozoa	HPF	63	87	149	64	79	20	79	42	92	25
Katablepharis sp.	HNF	0	47	107	12	2	17	9	4	1	25
MALV group I	Para	80	64	50	205	94	15	47	53	63	34

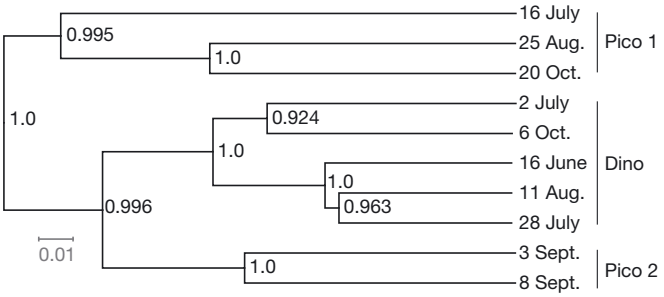

Fig. 4. Weighted UniFrac analysis of community similarity with jackknife coefficients shown at the nodes. Based on 1000 jackknife replicates on 1700 reads per sample. The summer samples were clustered into 3 community types: Pico 1, dominated by diverse mostly chlorophyte species; Pico 2, dominated by *Aureococcus anophagefferens*; and Dino, dominated by dinoflagellate reads

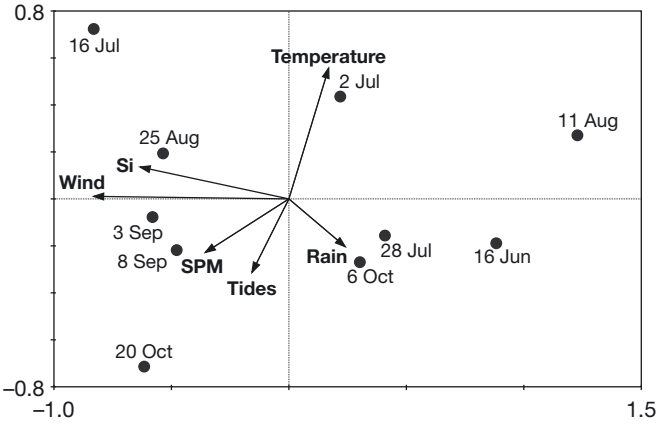

Fig. 5. Communities based on abundant ribotypes (see Table 2) distance-based redundancy analysis (dbRDA) biplot using forward selection on the environmental variables in Table 1. SPM: suspended particulates; Si: silicate; Wind: average wind over the preceding days; Temperature: temperature on the day of sampling; Rain: rain over the preceding days

The direction and significance of the dbRDA results were tested using Spearman's rank correlations of the variables that contributed to the dbRDA clustering. The proportion of dinoflagellate reads was negatively correlated with the FCM picoeuk concentration and phytoplankton, which were the reads binned as phototrophs and mixotrophs. High average wind speeds (over ca. 42 km h^{-1}) over the previous 5 d (Table 3) showed the greatest number of significant correlations, with higher average wind speeds negatively correlated with dinoflagellate reads and positively correlated with reads assigned to picophytoplankton and picoeuks. In addition, SPM and picoeuks were overall positively correlated with maximum wind events (Table 3).

Community trophic structure and potential interactions

The non-dinoflagellate reads were binned by likely trophic role based on literature searches of the taxa that were >98% similar to a known species (Table 2, Table S1 in the Supplement). The heterotrophic nanoflagellates (HNF) belonging to Telonemia, katablepharids, Cerozoa and various MAST clades changed little over the sampling period (Fig. 3). There were no significant correlations between proportions of HNF reads and bacterial concentrations

Table 3. Spearman rank correlation rho values comparing biological and environmental variables (n = 10 in all cases). Significant correlations ($p < 0.05$) are indicated in **bold**. First 3 variables are V4 reads summed from the binned categories (see 'Materials and methods; All phytoplankton [AllPhy], reads of picophytoplankton [PPP] and dinoflagellates [Dino] were from number); chlorophyll *a* (chl *a*), flow cytometry for eukaryotic picophytoplankton (picoeuks), temperature (T), salinity (Sal), silicate (Si), total suspended particulate matter (SPM), wind average (Wind avg) and maximum (Wind max.), rain average (Rain avg) and maximum (Rain max.) are from Table 1

	All Phy	PPP	Dino	Chl *a*	Pico-euks	T	Sal	Si	SPM	Wind avg	Wind max.	Rain avg	Rain max.
All Phy	1.00												
PPP	**0.99**	1.00											
Dino	**–0.94**	**–0.96**	1.00										
Chl *a*	–0.25	–0.29	0.35	1.00									
Picoeuks	**0.78**	**0.82**	**–0.86**	–0.32	1.00								
T	–0.13	0.01	0.18	0.05	0.19	1.00							
Sal	–0.22	–0.14	0.28	0.14	0.04	**0.93**	1.00						
Si	0.10	0.25	–0.03	0.09	0.25	**0.65**	0.46	1.00					
SPM	0.14	0.12	–0.09	0.44	0.47	0.43	0.39	0.28	1.00				
Wind avg	**0.68**	**0.65**	**–0.65**	0.01	**0.62**	–0.15	–0.17	0.05	0.37	1.00			
Wind max.	–0.40	–0.40	0.38	–0.31	**0.63**	–0.21	–0.17	–0.24	**–0.74**	**–0.79**	1.00		
Rain avg	–0.20	0.26	0.16	0.29	–0.46	–0.42	–0.24	–0.32	–0.32	–0.01	0.31	1.00	
Rain max.	0.23	–0.24	–0.19	–0.16	–0.46	0.41	0.23	0.37	0.40	0.01	–0.34	**–0.98**	1.00

(Spearman's rank correlation). Visually, the relative proportion of dinoflagellate reads alternated with reads that matched to picoeuk ribotypes (Table 3). A simple numerical experiment done using a 2-compartment model (phototrophs and dinoflagellates) with the addition of punctual events generated predator–prey type oscillations similar to the actual data (see text and Fig. S2 in the Supplement). Ciliates, which were the other major microzooplankton group with potential prey overlap with dinoflagellates, did not show any trends over the summer (Fig. 3).

DISCUSSION

Size and taxonomic changes in dominant groups

We found that picoeuks dominated cell abundance over much of the summer in the HAM. Concentrations fell in July and recovered after several wind events the third week of August. Since we found no consistent trend moving to smaller and smaller cells over the summer, our initial hypothesis was not supported. The use of HTS enabled us to identify the dominant ribotypes over the summer and highlighted the changing community composition.

The HAM lagoon has an estimated water residence time of 21 d (Guyondet & Koutitonsky 2008), and inflow from the Gulf of St. Lawrence may have contributed some species. For example, *Braarudosphaera* has been previously reported from the Gulf (Bérard-Therriault et al. 1999) so the Gulf could have been the source of the *Braarudosphaera*-like ribotype. However for the most part, picoeuk ribotypes tended to be very different from those found in the Atlantic- and Arctic-derived currents that contribute to the phytoplankton species composition of this region (Bérard-Therriault et al. 1999, Dasilva et al. 2014). The occurrence of small species used in aquaculture (e.g. *Nannochloris-Picochorum* and *Ostreococcus lucimarinus*) argues for locally selected flora in the shallow lagoon over much of the summer.

Nutrient limitation and bottom-up influences

Phytoplankton biomass as indicated by chl *a* concentrations nearly doubled (from ca. 1 to 2 µg l^{-1}) on 28 July, suggesting that either new or regenerated nutrients were added to the water column. The Magdalen Islands are in the middle of the Gulf of St. Lawrence and precipitation is considered the primary source of nitrate to the HAM (Guyondet & Koutitonsky 2008). Rain was not statistically associated with community changes (Fig. 5) and taxonomic makeup of the community argues against nitrate being a primary source of N into the lagoon in summer since diatoms, which have an advantage when nitrate is abundant (Seeyave et al. 2009, Glibert et al. 2016), were mostly absent. However, in low nutrient systems, nutrient levels are likely to remain low following nutrient pulses because they are rapidly taken up by phytoplankton (Glibert et al. 2016). Any nitrate pulses would be difficult to capture without constant monitoring, and the possibility of new nitrogen periodically entering the lagoons cannot be ruled out.

The increase in picoeuks was correlated with wind, and the chl *a* increases may have been fueled by N release from the sediments in this shallow lagoon. Ammonium concentrations in the water column are usually below the detection limits of standard methods (Robert et al. 2013) and because of these difficulties we did not measure ammonium concentrations over the summer, so input of ammonium remains a possibility. A benthocosm experiment was carried out in the same lagoon during our study and reported potential ammonium fluxes of ca. 54 µmol m^{-2} h^{-1} from anoxic sediment that had been loaded with mussel feces over several months (Robert et al. 2013). However, these conditions would apply to only the small area (5%) of the lagoon that is heavily impacted by aquaculture. In addition, we note that the HAM sediment is normally anoxic with a potentially active denitrifying community (Mohit et al. 2015) that, in undisturbed sediment, would be predicted to remove available nitrogen from the system.

Cyanobacterial concentrations were at their summer maximum on 3 September following the storm. The N:P ratio was consistent with a drawdown of P relative to N, suggesting potential diazotroph activity (Messer et al. 2015) from 3 to 8 September (Table 2). In a parallel study by Mohit et al. (2014), the dominant pelagic cyanobacteria were identified as *Synechococcus* and a phylotype related to *Gomphosphaeri*, neither of which are normally considered as nitrogen fixers. More intriguing was the post-storm occurrence on top of the sediment of the N_2 fixing cyanobacterium *Hydrocoleum*, and potentially diazotrophic sediment bacteria (Mohit et al. 2015). However, nitrogen fixation in the lagoon was not measured, and this source of N to the lagoon remains speculative. The planktonic bacterial community also changed following this storm event (Mohit et al. 2014) along with the increase in SPM (Table 1). The release of more complex organic mat-

ter from the sediments or the littoral zone following the storm (Mohit et al. 2014) may have supported *Aureococcus anophagefferens*, which is associated with high organic nutrients in coastal zones (Frischkorn et al. 2014).

Top-down control on small phytoplankton

Data collected from benthocosms and modeling Cherif et al. (2016) suggested that nutrient recycling sustains microbial food webs in the HAM lagoon, supporting dinoflagellates and ciliate populations (protist microzooplankton; Revelante & Gilmartin 1983, Dupuy et al. 1999), which can be a major food source for mesozooplankton and shellfish (Sherr & Sherr 1994, 2002, Trottet et al. 2007). Microzooplankton have multiple trophic roles and graze on not only bacteria, but each other, nanophytoplankton (2 to 20 µm diameter) and picophytoplankton (0.2 to 2 µm diameter) (Rassoulzadegan et al. 1988). An earlier study based on microscopy reported that ciliates dominated the microzooplankton in the adjacent Grande Entrée Lagoon (Trottet et al. 2007), which was in contrast with our study where, at least from the relative read count, dinoflagellates were more likely the dominant microzooplankton. Dinoflagellates, including HAB species, are thought to be favored by water column stability (Berman & Shteinman 1998), and the high proportion of dinoflagellate ribotypes could have been unexpected in this highly wind-influenced lagoon. However, tolerance to sheer stress may be species-specific; for example, *Gymnodinium catenatum* (Sullivan et al. 2003) and an undescribed *Gymnodinium* sp. (Berdalet et al. 2007) grow well under turbulent conditions. Our results suggest that the HAM dinoflagellates tolerate turbulence, but that high sustained wind has a negative impact.

In the nutrient-limited lagoon, the picophytoplankton increased during periods of higher winds consistent with disrupted grazer activity (Dugenne et al. 2014). In contrast, the decrease in picophytoplankton corresponded to periods of lower average winds consistent with meteorological forcing (Malej et al. 1997). While nutrient drawdown could be an indirect consequence, the increases in dinoflagellates would be consistent with higher predation during the relatively calm periods. The most frequent dinoflagellate ribotype was assigned to *Gyrodinium helveticum*, which was originally described from freshwater. However, although the 18S rRNA was closest to *G. helveticum*, this species is also phylogenetically very close to *G. rubrum* (Takano & Horiguchi 2004), which is marine. The species complex could possibly be mixotrophic, and the original description of *G. helveticum* suggested it was heterotrophic (Popovský 1982), making this ribotype a good candidate as a major picophytoplankton grazer.

Other species

The only described species of *Braarudosphaera*, *B. bigelowii*, is 2.4 to 7.2 µm (Konno et al. 2007) and has been previously reported from the Gulf of St. Lawrence (Bérard-Therriault et al. 1999). *Braarudosphaera* can host a cyanobacterial endosymbiont from the UCYN-A clade, which is reported to fix nitrogen (Thompson et al. 2012). Such a host–symbiont pair would have an advantage under nitrogen-limiting conditions. While UCYN-A was not detected in the parallel study of bacteria and cyanobacteria in the lagoon (Mohit et al. 2014), UCYN-A specific primers were not tested, and potential associations between the *Braarudosphaera*-like ribotype and cyanobacteria requires further investigation.

The second major peak of picoeuks on 25 August was associated with *Nannochloris* and *Picochlorum* spp. These 2 genera are very closely related and in need of taxonomic clarification (www.algaebase.org/; accessed 14 July 2016). *Picochlorum* and *Nannochloris* are frequently fed to shellfish larvae used in commercial aquaculture (https://ncma.bigelow.org/), and thus may have been introduced. However, we failed to find documentary evidence of their use in HAM, and their occurrence in summer is inconsistent with the normal mussel management practices in the lagoon, suggesting that they are established residents.

New species records and HAB events are thought to be increasing in coastal regions (Kennish et al. 2014). The presence of HAB species — including *A. anophagefferens*, which had high relative abundance on 3 and 8 September — suggests that the lagoon system could be sensitive to HAB events. The *A. anophagefferens* peak may have been related to high inputs of organic nitrogen from the sediment following the storm (see above). Another indication of potential for an HAB event was seen on 6 October, with *Karenia mikimotoi* among the abundant ribotypes and chl *a* concentrations 10-fold greater than before or after that date. *K. mikimotoi* is considered a red tide dinoflagellate in Domain II of Margalef's mandala (Wyatt 2014) when nutrients from unspecified sources are high but turbulence low. In the case of the 6 October sample, the autumn bloom may have been driven by

release of nutrients from senescent macrophyte beds along the shore (Drouin et al. 2012), but our sampling frequency could not resolve this and thus any source of nutrients remains unknown.

The last picoeuk peak on 20 October included *Ostreococcus*. This genus was originally isolated from aquaculture lagoons in the Mediterranean but appears to be absent from coastal waters off Nova Scotia and is rare in coastal Atlantic waters (Dasilva et al. 2014), presumably because of a preference for warmer water. The occurrence of *Ostreococcus* in October when temperatures were coolest could suggest a wider temperature tolerance (Demir-Hilton et al. 2011). This species may have also arrived in the lagoon as a result of human introduction and aquiculture activity. Unfortunately, historical records for all of these small species are lacking, and the role of human introductions even in this isolated region will be difficult to test.

Over the sampling period the putative parasite (MALV group 1) co-occurred at high relative abundance with a possible host (*G. helveticum*), and although more frequent sampling would be required to establish any interaction (Siano et al. 2011), its presence suggests complex trophic interactions could be occurring when dinoflagellates were abundant in July and early August.

CONCLUSIONS

We found that in this closed lagoon, which has little exchange with surrounding oceanic waters, there was no downward trend in the size structure of the plankton recorded from flow cytometry over the summer. Rather, concentrations of picoeukaryotes fluctuated over the summer and the relative abundance of species changed frequently. Overall, wind, which is an extrinsic process, was the most significant factor associated with changes in the abundance of eukaryotic picophytoplankton, with periods of high average wind favoring smaller cells. We speculate that the trophic interactions with dinoflagellates and other heterotrophic microbial eukaryotes exerted periodic control on picoeukaryotes when wind fields lessened. In summary, wind may have a first order effect on grazing, a second order effect by increasing direct nutrient release or even third order effects as seen in the temporary establishment of nitrogen-fixing cyanobacteria following a major storm. Overall, this suggests that increasing high wind events could have consequences on coastal phytoplankton species composition.

Acknowledgements. We thank N. Toupoint and L. Solomon for aid in the field and laboratory; A. Monier for bioinformatics advice on UniFrac; and P. Archambault and C. McKindsey for valuable discussions. This study was carried out as part of a Natural Sciences and Engineering Research Council of Canada (NSERC) funded Strategic Grant: 'Integrating across scales in marine aquaculture: the role of trophic dynamics and nutrient recycling for mussel production', with G. Fussman as lead. Additional support from the Fonds de Recherche du Québec (FQRNT), Québec Ocean and Centre d'Innovation de l'Aquaculture et des Pêches du Québec (Merinov) were essential for the completion of this study.

LITERATURE CITED

Adl SM, Simpson AGB, Lane CE, Lukeš J and others (2012) The revised classification of eukaryotes. J Eukaryot Microbiol 59:429–493

Aljanabi SM, Martinez I (1997) Universal and rapid salt-extraction of high quality genomic DNA for PCR-based techniques. Nucleic Acids Res 25:4692–4693

Altschul SF, Gertz EM, Agarwala R, Schaffer AA, Yu YK (2009) PSI-BLAST pseudocounts and the minimum description length principle. Nucleic Acids Res 37:815–824

Anglès S, Jordi A, Campbell L (2015) Responses of the coastal phytoplankton community to tropical cyclones revealed by high-frequency imaging flow cytometry. Limnol Oceanogr 60:1562–1576

Arvola L (1981) Spectrophotometric determination of chlorophyll *a* and phaeopigments in ethanol extractions. Ann Bot Fenn 18:221–227

Balzer S, Malde K, Lanzén A, Sharma A, Jonassen I (2010) Characteristics of 454 pyrosequencing data — enabling realistic simulation with FlowSim. Bioinformatics 26: i420–i425

Belzile C, Brugel S, Nozais C, Gratton Y, Demers S (2008) Variations of the abundance and nucleic acid content of heterotrophic bacteria in Beaufort Shelf waters during winter and spring. J Mar Syst 74:946–956

Bérard-Therriault L, Poulin M, Bossé L (1999) Guide d'identification du phytoplancton marin de l'estuaire et du golfe du Saint-Laurent incluant également certains protozoaires. Canadian Special Publication of Fisheries and Aquatic Sciences, NRC Research Press, Ottawa

Berdalet E, Peters F, Koumandou VL, Roldán C, Guadayol Ò, Estrada M (2007) Species-specific physiological response of dinoflagellates to quantified small-scale turbulence. J Phycol 43:965–977

Berman T, Shteinman B (1998) Phytoplankton development and turbulent mixing in Lake Kinneret (1992–1996). J Plankton Res 20:709–726

Blackford BL (1978) Wind-driven inertial currents in the Magdalen Shallows, Gulf of St. Lawrence. J Phys Oceanogr 8:653–664

Blazewicz SJ, Barnard RL, Daly RA, Firestone MK (2013) Evaluating rRNA as an indicator of microbial activity in environmental communities: limitations and uses. ISME J 7:2061–2068

Canton M, Anschutz P, Poirier D, Chassagne R, Deborde J, Savoye N (2012) The buffering capacity of a small estuary on nutrient fluxes originating from its catchment (Leyre estuary, SW France). Estuar Coast Shelf Sci 99: 171–181

Caporaso JG, Kuczynski J, Stombaugh J, Bittinger K and others (2010) QIIME allows analysis of high-throughput community sequencing data. Nat Methods 7:335–336

Caron DA, Hutchins DA (2013) The effects of changing climate on microzooplankton grazing and community structure: drivers, predictions and knowledge gaps. J Plankton Res 35:235–252

Cherif M, Granados M, Duffy S, Robert P and others (2016) Potential for local fertilization: a benthocosm test of long-term and short-term effects of mussel excretion on the plankton. PLOS ONE 11:e0156411

Cock PJA, Antao T, Chang JT, Chapman BA and others (2009) Biopython: freely available Python tools for computational molecular biology and bioinformatics. Bioinformatics 25:1422–1423

Comeau AM, Li WKW, Tremblay JÉ, Carmack EC, Lovejoy C (2011) Arctic ocean microbial community structure before and after the 2007 record sea ice minimum. PLOS ONE 6:e27492

Dasilva CR, Li WKW, Lovejoy C (2014) Phylogenetic diversity of eukaryotic marine microbial plankton on the Scotian Shelf, Northwestern Atlantic Ocean. J Plankton Res 36:344–363

Demir-Hilton E, Sudek S, Cuvelier ML, Getemann CL, Zehr JP, Worden AZ (2011) Global distribution patterns of distinct clades of the photosynthetic picoeukaryote *Ostreococcus.* ISME J 5:1095–1107

Drouin A, McKindsey CW, Johnson LE (2012) Detecting the impacts of notorious invaders: experiments versus observations in the invasion of eelgrass meadows by the green seaweed *Codium fragile.* Oecologia 168:491–502

Dugenne M, Thyssen M, Nerini D, Mante C and others (2014) Consequence of a sudden wind event on the dynamics of a coastal phytoplankton community: an insight into specific population growth rates using a single cell high frequency approach. Front Microbiol 5:485

Dupuy C, Le Gall S, Hartmann HJ, Breret M (1999) Retention of ciliates and flagellates by the oyster *Crassostrea gigas* in French Atlantic coastal ponds: protists as a trophic link between bacterioplankton and benthic suspension-feeders. Mar Ecol Prog Ser 177:165–175

Dupuy C, Ryckaert M, LeGall S, Hartmann HJ (2007) Seasonal variations in planktonic community structure and production in an Atlantic coastal pond: the importance of nanoflagellates. Microb Ecol 53:537–548

Edgar RC, Haas BJ, Clemente JC, Quince C, Knight R (2011) UCHIME improves sensitivity and speed of chimera detection. Bioinformatics 27:2194–2200

Flynn KJ, Stoecker DK, Mitra A, Raven JA and others (2013) Misuse of the phytoplankton–zooplankton dichotomy: the need to assign organisms as mixotrophs within plankton functional types. J Plankton Res 35:3–11

Frischkorn KR, Harke MJ, Gobler CJ, Dyhrman ST (2014) De novo assembly of *Aureococcus anophagefferens* transcriptomes reveals diverse responses to the low nutrient and low light conditions present during blooms. Front Microbiol 5:375

Gilmartin M, Revelante N (1978) The phytoplankton characteristics of the barrier island lagoons of the Gulf of California. Estuar Coast Mar Sci 7:29–47

Glibert PM (2016) Margalef revisited: a new phytoplankton mandala incorporating twelve dimensions, including nutritional physiology. Harmful Algae 55:25–30

Glibert PM, Wilkesron FP, Dugdale RC, Raven JA and others (2016) Pluses and minuses of ammonium and nitrate uptake and assimilation by phytoplankton and implications for productivity and community composition, with emphasis on nitrogen-enriched conditions. Limnol Oceanogr 61:165–197

Grasshoff K, Kremling K, Ehrhardt M (eds) (2009) Methods of seawater analysis. John Wiley & Sons, Hoboken, NJ

Guadayol Ò, Peters F, Marrasé C, Gasol JM and others (2009) Episodic meteorological and nutrient-load events as drivers of coastal ecosystem dynamics: a time series analysis. Mar Ecol Prog Ser 381:139–155

Guyondet T, Koutitonsky VG (2008) Tidal and residual circulations in coupled restricted and leaky lagoons. Estuar Coast Shelf Sci 77:396–408

Harding T, Jungblut AD, Lovejoy C, Vincent WF (2011) Microbes in high Arctic snow and implications for the cold biosphere. Appl Environ Microbiol 77:3234–3243

Hochberg Y (1988) A sharper Bonferroni procedure for multiple tests of significance. Biometrika 75:800–803

Hugerth LW, Muller EEL, Hu YOO, Lebrun LAM and others (2014) Systematic design of 18S rRNA gene primers for determining eukaryotic diversity in microbial consortia. PLOS ONE 9:e95567

Kennish MJ, Brush MJ, Moore KA (2014) Drivers of change in shallow coastal photic systems: an introduction to a special issue. Estuaries Coasts 37(Suppl 1):3–19

Konno S, Harada N, Narita H, Jordan RW (2007) Living *Braarudosphaera bigelowii* (Gran & Braarud) Deflandre in the Bering Sea. J Nannoplankton Res 29:78–87

Koutitonsky VG (2005) Modélisation numérique intégrée des courants, des vagues et du transport des sédiments à l'entrée de la lagune de Havre-aux-Maisons. Rapport de recherche LHE-05-2. Institut des Sciences de la Mer de Rimouski, Rimouski

Koutitonsky VG, Navarro N, Booth D (2002) Descriptive physical oceanography of great-entry lagoon, Gulf of St. Lawrence. Estuar Coast Shelf Sci 54:833–847

Lovejoy C, Legendre L, Martineau MJ, Bâcle J, von Quillfeldt CH (2002) Distribution of phytoplankton and other protists in the North Water. Deep Sea Res II 49: 5027–5047

Lovejoy C, Comeau A, Thaler M (2015) Curated reference database of SSU rRNA for northern marine and freshwater communities of Archaea, Bacteria and microbial eukaryotes, v. 1.0. Nordicana D23

Luddington IA, Kaczmarska I, Lovejoy C (2012) Distance and character-based evaluation of the V4 region of the 18S rRNA gene for the identification of diatoms (Bacillariophyceae). PLOS ONE 7:e45664

Malej A, Mozeti P, Mala V, Turk V (1997) Response of summer phytoplankton to episodic meteorological events (Gulf of Trieste, Adriatic Sea). Mar Ecol 18:273–288

Messer LF, Doubell M, Jeffries TC, Brown MV, Seymour JR (2015) Prokaryotic and diazotrophic population dynamics within a large oligotrophic inverse estuary. Aquat Microb Ecol 74:1–15

Mohit V, Archambault P, Toupoint N, Lovejoy C (2014) Phylogenetic differences in summer attached and free-living bacterial communities in a temperate coastal lagoon, revealed via high throughput 16S rRNA gene sequencing. Appl Environ Microbiol 80:2071–2083

Mohit V, Archambault P, Lovejoy C (2015) Resilience and adjustments of surface sediment bacterial communities in an enclosed shallow coastal lagoon, Magdalen Islands, Gulf of St. Lawrence, Canada. FEMS Microbiol Ecol 91: fiv038

Moisan N, Bourque F, Lachance AA (2012) Monitoring en mytiliculture au Québec en 2009. Rapport de RD no. 12-09, Merinov, Grande-Rivière

Myrand B, Gaudreault J (1996) Summer mortality of blue mussels (*Mytilus edulis* Linneaus, 1758) in the Magdalen Islands (southern Gulf of St. Lawrence, Canada). J Shellfish Res 14:395–404

Pennock JR (1985) Chlorophyll distributions in the Delaware Estuary: regulation by light-limitation. Estuar Coast Shelf Sci 21:711–725

Pérez-Ruzafa A, Fernández AI, Marcos C, Gilabert J, Quispe JI, García-Charton JA (2005) Spatial and temporal variations of hydrological conditions, nutrients and chlorophyll *a* in a Mediterranean coastal lagoon (Mar Menor, Spain). Hydrobiologia 550:11–27

Popovský J (1982) Another case of phagotrophy by *Gymnodinium helveticum* PENARD f. *Achroum* SKUJA. Arch Protistenkd 125:73–78

Price MN, Dehal PS, Arkin AP (2010) FastTree 2 — approximately maximum-likelihood trees for large alignments. PLOS ONE 5:e9490

Rassoulzadegan F, Laval-Peuto M, Sheldon RW (1988) Partitioning of the food ration of marine ciliates between pico- and nanoplankton. Hydrobiologia 159:75–88

Raven JA (1998) The twelfth Tansley Lecture. Small is beautiful: the picophytoplankton. Funct Ecol 12:503–513

Record NR, Pershing AJ, Runge JA, Mayo CA, Monger BC, Chen C (2010) Improving ecological forecasts of copepod community dynamics using genetic algorithms. J Mar Syst 82:96–110

Revelante N, Gilmartin M (1983) Microzooplankton distribution in the Northern Adriatic Sea with emphasis on the relative abundance of ciliated protozoans. Oceanol Acta 6:407–415

Robert P, Mckindsey CW, Chaillou G, Archambault P (2013) Dose-dependent response of a benthic system to biodeposition from suspended blue mussel (*Mytilus edulis*) culture. Mar Pollut Bull 66:92–104

Roy S, Mayzaud P, Souchu P (1991) Environnement physico-chimique et trophique d'un site mytilicole aux Îles-de-la-Madeleine (Québec). II. Matière particulaire, composition biochimique et productivité primaire. Publ Spec Can Sci Halieut Aquat 113:219–230

Saldarriaga JF, Cavalier-Smith T, Menden-Deuer S, Keeling PJ (2004) Molecular data and the evolutionary history of dinoflagellates. Eur J Protistol 40:85–111

Schapira M, Vincent D, Gentilhomme V, Seuront L (2008) Temporal patterns of phytoplankton assemblages, size spectra and diversity during the wane of a *Phaeocystis globosa* spring bloom in hydrologically contrasted coastal waters. J Mar Biol Assoc UK 88:649–662

Schloss PD, Westcott SL, Ryabin T, Hall JR and others (2009) Introducing mothur: open-source, platform-independent, community-supported software for describing and comparing microbial communities. Appl Environ Microbiol 75:7537–7541

Seeyave S, Probyn TA, Pitcher GC, Lucas MI, Purdie DA (2009) Nitrogen nutrition in assemblages dominated by *Pseudo-nitzschia* spp., *Alexandrium catenella* and *Dinophysis acuminata* off the west coast of South Africa. Mar Ecol Prog Ser 379:91–107

Sherr EB, Sherr BF (1994) Bacterivory and herbivory: key roles of phagotrophic protists in pelagic food webs. Microb Ecol 28:223–235

Sherr EB, Sherr BF (2002) Significance of predation by protists in aquatic microbial food webs. Antonie Van Leuwenhoek 81:293–308

Siano R, Montresor M, Probert I, Not F, de Vargas C (2010) *Pelagodinium* gen. nov. and *P. béii* comb. nov., a dinoflagellate symbiont of planktonic foraminifera. Protist 161:385–399

Siano R, Alves-de-Souza C, Foulon E, Bendif EM, Simon N, Guillou L, Not F (2011) Distribution and host diversity of Amoebophryidae parasites across oligotrophic waters of the Mediterranean Sea. Biogeosciences 8:267–278

Souchu P, Mayzaud P (1991) Inorganic nutrients in precipitation over the Magdalen Islands area (Quebec, Canada) and their impact on the primary productivity of the lagoons. Atmos Res 26:543–554

Sullivan JM, Swift E, Donaghay PL, Rines JE (2003) Small-scale turbulence affects the division rate and morphology of two red-tide dinoflagellates. Harmful Algae 2:183–199

Takano Y, Horiguchi T (2004) Surface ultrastructure and molecular phylogenetics of four unarmored heterotrophic dinoflagellates, including the type species of the genus *Gyrodinium* (Dinophyceae). Phycol Res 52: 107–116

Taylor FJ (1976) Flagellate phylogeny: a study in conflicts. J Protozool 23:28–40

ter Braak CJF, Smilauer P (1998) CANOCO reference manual and user's guide to CANOCO for Windows: software for canonical community ordination (version 4.5). Microcomputer Power, Ithaca, NY

Thompson AW, Foster RA, Krupke A, Carter BJ and others (2012) Unicellular cyanobacterium symbiotic with a single-celled eukaryotic alga. Science 337:1546–1550

Trottet A, Roy S, Tamigneaux E, Lovejoy C (2007) Importance of heterotrophic planktonic communities in a mussel culture environment: the Grande Entrée Lagoon, Magdalen Islands (Québec, Canada). Mar Biol 151: 377–392

Vaulot D, Eikrem W, Viprey M, Moreau H (2008) The diversity of small eukaryotic phytoplankton (≤3 µm) in marine ecosystems. FEMS Microbiol Rev 32:795–820

Wright SW, Jeffrey SW, Mantoura RFC (2005) Phytoplankton pigments in oceanography: guidelines to modern methods. UNESCO Publishing, Paris

Wyatt T (2014) Margalef's mandala and phytoplankton bloom strategies. Deep-Sea Res II 101:32–49

Yeo SK, Huggett MJ, Eiler A, Rappé MS (2013) Coastal bacterioplankton community dynamics in response to a natural disturbance. PLOS ONE 8:e56207

Editorial responsibility: Robert Sanders, Philadelphia, Pennsylvania, USA

Submitted: July 19, 2016; Accepted: January 9, 2017
Proofs received from author(s): February 26, 2017